Core and valence exciton formation in x-ray absorption, x-ray emission and x-ray excited optical luminescence from passivated Si nanocrystals at the Si $L_{2,3}$ edge



2009 J. Phys.: Condens. Matter 21 095005

(http://iopscience.iop.org/0953-8984/21/9/095005)

J. Phys.: Condens. Matter **21** (2009) 095005 (8pp) doi:10.1088/0953-8984/21/9/095005

# Core and valence exciton formation in x-ray absorption, x-ray emission and x-ray excited optical luminescence from passivated Si nanocrystals at the Si $L_{2,3}$ edge

**L Šiller[1,5], S Krishnamurthy[1], L Kjeldgaard[2], B R Horrocks[3], Y Chao[3], A Houlton[3], A K Chakraborty[4] and M R C Hunt[4]**

[1] School of Chemical Engineering and Advanced Materials, University of Newcastle upon Tyne, Newcastle upon Tyne NE1 7RU, UK
[2] MAXLAB, Lund University, S-22100 Lund, Sweden
[3] School of Natural Sciences, University of Newcastle upon Tyne, Newcastle upon Tyne NE1 7RU, UK
[4] Department of Physics, University of Durham, Durham DH1 3LE, UK

E-mail: Lidija.Siller@ncl.ac.uk

Received 8 September 2008, in final form 18 December 2008
Published 30 January 2009
Online at stacks.iop.org/JPhysCM/21/095005

**Abstract**
Resonant inelastic x-ray scattering (RIXS), x-ray absorption spectroscopy and x-ray excited optical luminescence (XEOL) have been used to measure element specific filled and empty electronic states over the Si $L_{2,3}$ edge of passivated Si nanocrystals of narrow size distribution (diameter $2.2 \pm 0.4$ nm). These techniques have been employed to directly measure absorption and luminescence specific to the local Si nanocrystal core. Profound changes occur in the absorption spectrum of the nanocrystals compared with bulk Si, and new features are observed in the nanocrystal RIXS. Clear signatures of core and valence band exciton formation, promoted by the spatial confinement of electrons and holes within the nanocrystals, are observed, together with band narrowing due to quantum confinement. XEOL at 12 K shows an extremely sharp feature at the threshold of orange luminescence (i.e., at $\sim$1.56 eV (792 nm)) which we attribute to recombination of valence excitons, providing a lower limit to the nanocrystal band gap.

## 1. Introduction

The electronic structure and electron dynamics of semiconductor clusters and nanocrystals is a topic of very high current interest, see for example [1–3]. Over the past decade, there has been continued interest in Si nanostructures, especially porous Si (por-Si) and ultrafine Si particles exhibiting visible luminescence due to quantum confinement [4–6]. The effects of confinement can be directly studied by mapping the electronic structure of nanostructured Si. Scanning tunnelling spectroscopy has been employed to measure the total density of states (DOS) of size selected Si clusters [7], but this technique is limited to energies close to the Fermi level. Photoemission or electron absorption techniques suffer from sensitivity to interface chemistry and charging [8]. In the gas phase, photoemission measurements from Si cluster anions have been obtained, but only for the first 4 eV of the valence band [9]. X-ray emission spectroscopy (XES) is a powerful technique for investigating the local, element specific, partial density of states (LPDOS) [10, 11] of solids and has advantages over photoemission spectroscopy because of the large probe depth, relative insensitivity to heterogeneous surface species, and insensitivity to charging [10, 11]. By tuning the photon energy to the appropriate absorption edge (resonant

[5] Author to whom any correspondence should be addressed.

 

inelastic x-ray scattering, or RIXS), chemical specificity is possible, which is invaluable in heterogeneous systems such as nanocrystallites passivated by a surface species or embedded in a matrix. However, excitonic effects in RIXS can complicate the interpretation of spectra. This is because, with excitation energies close to the elemental edge, the final states of the measured RIXS spectrum are low energy valence excitations and dynamical effects on the femtosecond timescale may dominate the x-ray emission process (for a review on the dynamic phenomena in RIXS, see for example [12]). When the excitation energies are above the absorption edge, the x-ray emission spectrum can be described as a two step process of simple absorption and de-excitation, without some additional interference channel, and therefore the measured spectra represent the partial density of states governed by dipole selection rule; this process is normally called XES in the literature.

XES has previously been used to study por-Si [13], Si nanocrystals produced by evaporation in an argon buffer gas [14], Si nanocrystals embedded in a $SiO_2$ matrix formed by Si ion implantation [15], Si nanocrystals produced by a laser vaporization controlled condensation technique [16] and very recently matrix-embedded Si nanoclusters formed upon annealing $SiO/SiO_2$ superlattices [17]. However, in these previous studies the picture has, in general, been complicated due to the presence of a significant fraction of $SiO_x$ in the samples and/or a large size distribution in the nanostructures when compared with the work reported here. In consequence, it can be argued that definitive measurements of the LPDOS of Si nanocrystals are still lacking, although theoretical studies have been performed [18, 19].

In this work we report measurements on free standing Si nanocrystals with a narrow size distribution [20, 21]. RIXS [12] at the Si $L_{2,3}$ edge is used to avoid the strong contribution from oxides observed in non-resonant measurements of the LPDOS. X-ray excited optical luminescence (XEOL) is also a 'photon in–photon out' technique and spectra reveal the states involved in radiative de-excitation processes. XEOL is site and excitation channel specific when the excitation energy is tuned across the x-ray absorption edge of atoms whose local electronic structure is coupled to the luminescence channel [22, 23]. In this work XEOL above the Si $L_{2,3}$ edge has been used to obtain a lower limit to the Si nanocrystal band gap: the energy and temperature dependence of these features have been published elsewhere [24].

## 2. Experimental details

The Si nanocrystals used in this work were produced by a technique described elsewhere [20, 21]. The nanocrystals are passivated by Si–$CH_2$–R (n-alkyl) surface groups to prevent aggregation and reaction with the ambient environment (although a small amount of suboxide is present at the surface of the nanocrystals) [8]. The novelty of our samples is that it is possible to produce Si nanocrystals which are air-stable with narrow size distribution in milligramme quantities [20, 21], which is a requirement for many spectroscopic techniques. The size distribution of the nanocrystals has been measured with scanning tunnelling microscopy [8], x-ray diffraction (XRD) [21], small angle x-ray scattering [21], aberration-corrected scanning transmission electron microscopy (SuperSTEM) [21] and Raman spectroscopy [21], these measurements demonstrate that the silicon core is crystalline. The average diameter of the core (plus submonolayer $SiO_x$) of the nanocrystals studied in this report was found to be $2.2 \pm 0.4$ nm [21].

We calculated the amount of (sub)oxide present in our SiNCs from the integrated absorbances of the peaks due to Si–O stretches and methyl stretching modes in normal transmission FTIR spectra, and the oscillator strengths computed by *ab initio* calculations on small molecule models (MP2/6-311++G(d, p)) [25]. For a typical sample, the ratio of integrated absorbances was 1.0:0.78; after normalizing by the ratio of oscillator strengths, we estimate the coverage of oxide to be 13% of the coverage of alkyl chains. It is well-known that the alkyl chain coverage does not exceed about 50% on silicon due to steric reasons [26, 27], therefore the FTIR data is consistent with a small amount of suboxide, amounting to about 7% of the surface Si atoms.

The x-ray absorption spectroscopy (XAS) and XES measurements were performed at beamline I511-1, MAXLab, Lund, Sweden. X-ray emission was detected using a grazing incidence Rowland spectrometer [28]. We used a 300 l $mm^{-1}$, 3 m radius grating with a 40 $\mu$m entrance slit and experimentally determined the resolution to be 0.25 eV, by measuring the full width at half maximum (FWHM) of the elastic peak. The resolution of the monochromator was set so that the incident photon beam had an energy resolution of 0.1 eV. X-ray absorption spectroscopy was performed by measuring the partial photon yield (PPY) across the Si L edge using a micro channel plate detector (MCP). PPY rather than the total photon yield (TPY) from the sample was used in order to avoid the influence of sample reflectivity on the measurement. Chamber pressures were maintained below $1 \times 10^{-10}$ mbar and data were obtained at room temperature. The photoluminescence excitation and emission spectra were acquired with the mobile luminescence end station (MoLES) at beamline MPW6.1, CCLRC Daresbury Laboratory with samples measured at room temperature and at 12 K.

A suspension of silicon nanocrystals was produced by stirring a dry nanocrystal powder in dichloromethane, and several drops of this suspension were cast onto graphite (HOPG) or a gold foil. After evaporation of the solvent the substrate was rapidly introduced into an ultra-high vacuum (UHV) chamber containing the x-ray emission spectrometer. In a previous study [8] we found that by rapid introduction of the nanocrystals into UHV we could avoid beam-induced oxidation, which occurs due to photo-induced reaction with adsorbed water acquired during long-term storage of nanocrystal films in air. When silicon nanocrystal films are rapidly introduced into vacuum the only effect observed in photoelectron spectra is the charging effect [8], the elimination of which was one of the motivations for the use of 'photon in–photon out' techniques in this study.

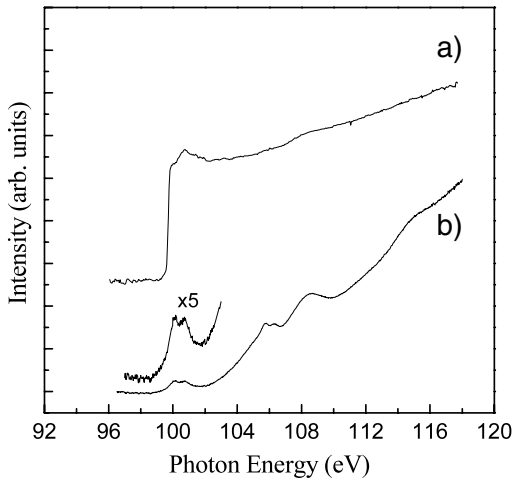


**Figure 1.** Si $L_{2,3}$ x-ray partial photon yield spectra of (a) bulk Si and (b) Si nanocrystals.

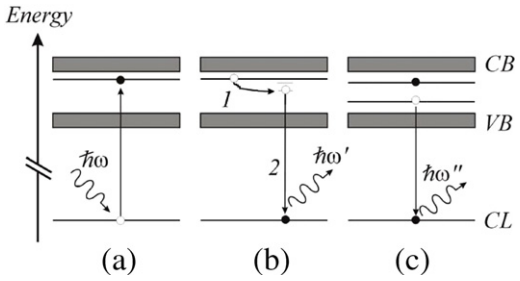


**Figure 2.** Schematic representations of (a) core exciton formation upon absorption of an x-ray photon: an electrostatic interaction between the promoted electron and the core level (CL) hole creates a state below the conduction band (CB) minimum in the excited system; (b) relaxation of the core exciton via coupling to lattice vibrations: emission of phonons (step 1) enables the excitonic state to relax to lower energy leading to the emission of an x-ray photon with energy less than that originally absorbed (step 2); (c) valence exciton formation during x-ray emission: an electron at the top of the valence band (VB) recombines with a core hole, and the resultant valence hole interacts with an electron in a conduction band (or core exciton) state forming a valence exciton. For clarity the energy levels are not drawn to scale.

## 3. Results and discussion

Figure 1 shows the partial photon yield (PPY) obtained from bulk Si (spectrum (a)) and passivated Si nanocrystals (spectrum (b)) at the Si $L_{2,3}$ edge. PPY provides a measure of the total x-ray absorption of the sample and does not suffer from the surface sensitivity of electron yield techniques or sample charging. Data for bulk silicon are in agreement with previous work [29, 30]. However, the absorption spectrum from the nanocrystals is remarkably different from both the bulk and what would be expected from a consideration of the theoretically determined unoccupied density of states in silicon clusters containing a few tens of atoms [18, 19]. The nanocrystal XAS consists of a single, relatively sharp, spin–orbit split peak superimposed upon a smooth background intensity between threshold and the onset of oxide-related absorption (bands at 106, 108 eV and a weak band at 115 eV which are commonly attributed to 'inner well resonances' of Si oxide [29, 31–33]). The relatively high strength of the oxide features in the XAS spectra of the silicon nanocrystals despite the 'bulk sensitive' PPY detection can be attributed to the structure of the nanocrystal film: passivation of the silicon nanocrystal surfaces by alkyl groups prevents their sintering, thus the film consists of individual nanoparticles each with their own surface (including suboxides) distributed throughout the bulk of the film. Therefore, in contrast to a bulk silicon sample with the same surface composition, a film of silicon nanocrystals with (limited) surface oxidation presents surface oxide throughout the film thickness, so increasing the oxide signal relative to a conventional solid silicon sample.

A broadening of absorption onset was observed by Eisebitt *et al* in XAS from porous Si [13], and attributed to the crystallite size distribution in their samples. However, in our spectra, which are from a sample with a well-defined and narrow diameter distribution [21], a clear 0.61 eV spin–orbit splitting [34] is observed in the PPY from the nanocrystals (magnified region of figure 1, curve b), whilst such splitting may be washed out by the size inhomogeneity in the porous Si crystallites [13]. Given that RIXS (discussed below) and a wide variety of other techniques [21] indicate a well-ordered crystalline silicon core, the changes in absorption onset observed in our Si nanocrystal sample are likely to be intrinsic to the nanocrystals rather than the product of disorder or of inhomogeneity.

Single-dot luminescence spectroscopy has been used to study the emission line width of individual silicon nanocrystals and these studies have confirmed that oxidized nanocrystals exhibit discrete energy levels rather than continuous bands [35]. Therefore, the simple quantum mechanical model of 'particle in the box', leads one to expect the increased the level spacing in nanocrystals compared to bulk and therefore the transition from Si $L_2$ and $L_3$ levels to the lowest excited state should be better resolved than in the bulk Si.

Although a sharp rise in x-ray absorption is observed in bulk silicon, a shallow onset has been theoretically predicted [34, 36], because the absorption threshold should be related to the conduction band minima s-like electronic states due to dipole selection rules. The steep rise in absorption in bulk Si at the $L_{2,3}$ threshold, which is much steeper than the predicted conduction band DOS, has been attributed to excitonic effects in core-electron transitions to the conduction band, with *bound* core excitons being of Wannier type [37]. The theoretically calculated radius of the core exciton at the $L_{2,3}$ edge in bulk Si is ∼1.6 nm [38], which agrees well with measured x-ray absorption photon yield [34, 39]. The radius of the elemental Si core of the nanocrystals studied in this work is, at $d/2 = 1.1 \pm 0.2$ nm [21], substantially smaller than the core exciton radius, hence x-ray absorption in the silicon core at threshold should favour an excitonic final state more tightly bound than the corresponding bulk exciton. In consequence, it is not unreasonable that core exciton formation, shown schematically in figure 2(a), dominates emission below the oxide edge, to a greater degree than in bulk Si, leading to an absorption spectrum which no longer directly reflects the

unoccupied DOS. Indeed, the dominance of a single spin–orbit split doublet at the onset of x-ray absorption in the nanocrystals suggests a narrow, well-defined core exciton state in this system.

In addition to gross differences in spectral shape between the XAS of bulk silicon and silicon nanocrystals we observe a small, and unexpected, apparent red shift in the absorption threshold in the nanocrystals (located at 99.3 ± 0.1 eV) when compared with bulk Si (99.6 ± 0.1 eV). This behaviour is in contrast to the blue shift that has been previously reported for porous Si [29, 40], for $SiO_2$/Si superlattices [41] and Si nanoclusters [14] and attributed to quantum confinement. A red shift has, however, been reported for 2 and 3 nm diameter silicon clusters formed upon annealing $SiO_2$ superlattices by Zimina *et al* [17], although changes in the absorption spectrum were much less pronounced than those reported in this work. Although no other evidence was provided to support this attribution, it was suggested that this red shift, smaller in magnitude than that observed here, was associated with core exciton formation, which would be consistent with the interpretation of the x-ray absorption spectra from our silicon nanocrystals (figure 1(b)) presented above.

XAS at the $L_2$ edge predominantly probes the nanocrystal core, but because of the small number of Si atoms in the core and their close proximity to the surface, an alternative suggestion for the red shift could be that it arises due to the presence of the surface, perhaps from some strain-induced structural relaxation. For example, a red shift has been observed for very small diamond clusters (diamondoids) [2] and it has been suggested in this case that the bulk-related unoccupied states do not exhibit any quantum confinement but they are influenced by the termination of the surface by CH and $CH_2$ groups.

In order to test the hypothesis that core exciton formation is involved in the red shift observed in XAS, rather than simply structural effects, we employed RIXS to probe the dynamics of x-ray absorption and emission. In figure 3, the tail of the elastic (participator or recombination)[6] RIXS peak is plotted for energies on (100.2 eV) and off (101.8 eV) resonance with the sharp doublet at the XAS threshold, with normalization to the inelastic background. It is clear from the spectra that the tail of the elastic line is strongly enhanced on resonance, in a similar manner to RIXS spectra obtained from graphite [42, 43] and diamond [42] at the C 1s core exciton energy. Theoretical work [44, 45] has shown that the formation of a strong tail to the elastic line in these carbon systems is associated with coupling of the core exciton state to the vibrational modes of the solids (the core exciton relaxes via phonon emission prior to recombination, which leads to the emission of an x-ray photon of lower energy than that initially absorbed, as shown schematically in figure 2(b)). This tail is suppressed off resonance. The similarity of the data presented in figure 3 with that from diamond [42] and graphite [42, 43] suggests a similar origin for the differences between the spectra on and off resonance with the absorption edge and supports the hypothesis of core exciton formation

[6] The centre of the elastic peak is attenuated by a beam stop to prevent saturation during measurement of inelastic features, and is thus not shown.

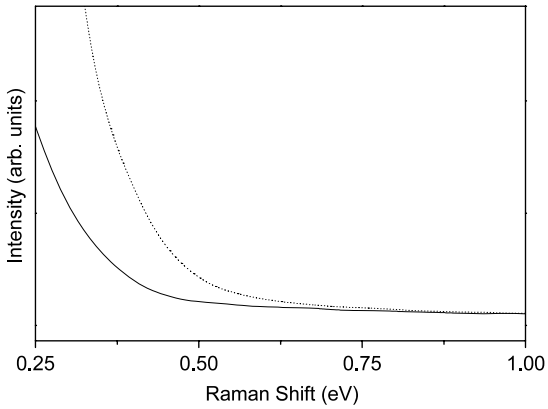


**Figure 3.** RIXS spectra showing the tail of the (quasi-) elastic or participator peak. The dashed line corresponds to an excitation energy of 100.20 eV and the full line to an excitation energy of 101.8 eV. The broadening of the elastic tail for the former excitation energy is characteristic of core exciton formation during the absorption–emission process.

for photon absorption at the Si $L_2$ and $L_3$ thresholds. It is notable, however, that the width of the 'quasi-elastic' tail is much smaller in figure 3 than that observed in either bulk diamond [42] or graphite [42, 43], where the tail extends for several electron-volts. The smaller tail in the quasi-elastic peak indicates that electron–phonon coupling in the silicon nanocrystal core exciton state is smaller than that in diamond and graphite. One potential explanation is that there is a reduced probability of electron–phonon relaxation (in particular acoustic phonon emission) in Si nanostructures compared with three-dimensional bulk solids such as graphite or diamond. Reduced electron–phonon relaxation rates, known in the literature as a 'phonon bottleneck' have been predicted for zero-dimensional semiconductor systems [46, 47] and this has been confirmed by time resolved differential transmission measurements in self-assembled InGaAs quantum dots [48]. An electron in an excited state cannot relax to the ground state by inelastic phonon scattering unless the energy level separation is exactly equal to the phonon energy (acoustic phonon emission plays the most important role), which is therefore likely to lead to a slow relaxation effect [46, 47].

XES data obtained at a range of excitation energies are presented in figure 4. The top spectrum was obtained at incident photon energy of 140.0 eV, well above the threshold: it therefore reflects the full PDOS of the nanocrystals and strongly resembles spectra from $SiO_2$ [49], as does the spectrum at 103.0 eV, which is already sensitive to surface oxides. The dominance of emission from oxides demonstrates the need for RIXS in order to probe the electronic structure of the elemental Si core. The spectrum obtained at an excitation energy of 102.0 eV, reflecting the Si core, is similar to that of bulk Si (figure 5(a)) and is significantly different from that of amorphous silicon [50], consistent with a crystalline structure in the silicon core [21].

As the excitation energy is reduced to the $L_2$ threshold at 100.7 eV, sharp features are observed on the sloping background of the elastic peak (figure 4, bottom curve,

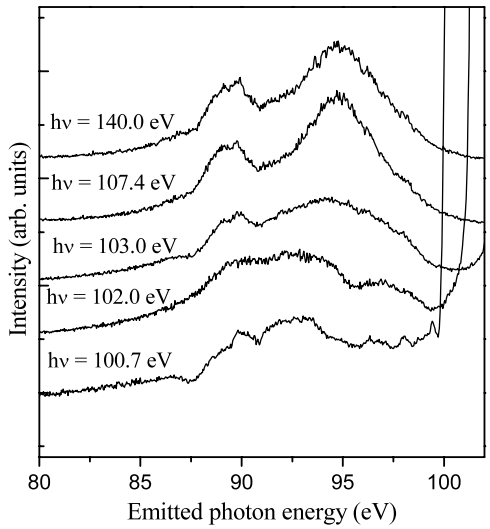


**Figure 4.** High resolution RIXS from Si nanocrystals obtained at 100.7, 102.0, 103.0, 107.4 and 140 eV excitation energies.

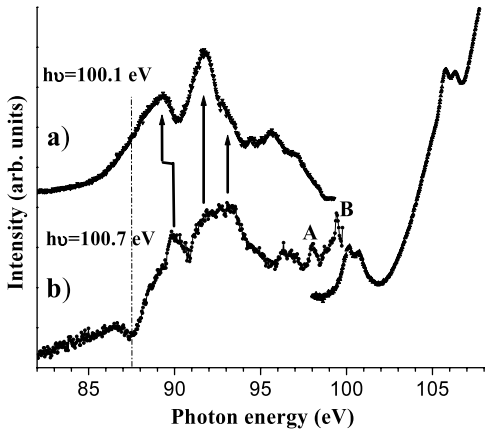


**Figure 5.** (a) High resolution RIXS of bulk Si obtained at the Si $L_2$ edge, $h\nu = 100.1$ eV (b) RIXS of passivated Si nanocrystals measured at the Si $L_2$ edge, $h\nu = 100.7$ eV. X-ray absorption data from figure 1(b) are plotted on the same energy scale in order to make comparison with unoccupied valence states. Arrows link spectral features of the nanocrystals and the bulk. The dotted line marks the upper end of the nanocrystal valence band.

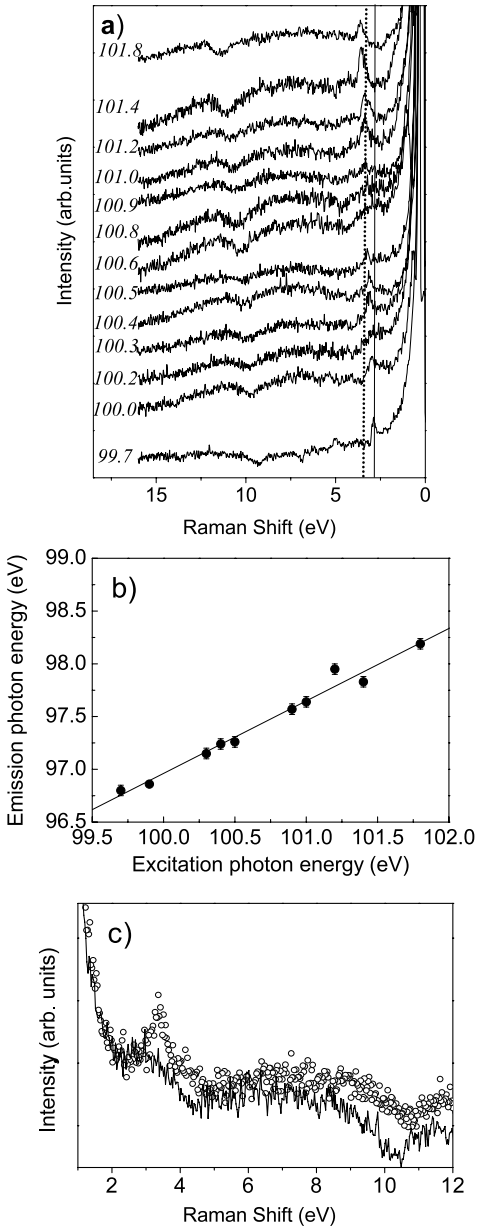


**Figure 6.** (a) High resolution RIXS from Si nanocrystals obtained at excitation energies of 99.7, 100.0, 100.2, 100.3, 100.4, 100.5, 100.6, 100.8, 100.9, 101.0, 101.2, 101.4, and 101.8 eV; (b) dispersion of peak A (see figure 5) obtained from figure 6(a); (c) expanded view of inelastic region of spectra excited at 101.4 eV (open circles) and 100.6 eV (solid line) showing the strong variation in intensity of the valence band exciton peak.

reproduced for greater clarity in figure 5). Two particularly sharp features are observed towards higher emission energies, labelled as peak A and peak B in figure 5, with the FWHM of peak B resolution limited at 0.25 eV. Peak A, located at $98.0 \pm 0.1$ eV, is at the edge of the valence band intensity observed in the RIXS spectrum whilst peak B, located at $99.40 \pm 0.02$ eV, is at significantly higher photon energy and overlaps with the XAS which is plotted on a common energy scale in figure 5.

To explore the origin of these sharp peaks we obtained RIXS spectra over the Si $L_{2,3}$ edge from a different sample using a fine excitation energy step (figure 6(a)). Peak A strongly varies in intensity with excitation energy, reaching maxima for excitation energies at the edges of the spin–orbit doublet seen at threshold in XAS (figure 1). It is clear from the spectra that peak A does not occur at fixed loss energy and hence is not a Raman loss. However, neither does peak A occurs at fixed emission energy, but disperses linearly (with a gradient of 0.68) over the excitation energy range, as shown in figure 6(b). Excitation of the carbon K-edge by third harmonic light, and third-order detection of the resultant emission can be ruled out since the resulting emission energies, obtained by dividing first-order emission [51] or absorption [52] energies by three do not correspond to the observed peak positions.

In RIXS, absorption and emission events can remain coupled in a fast coherent process in which the full momentum

is conserved even above threshold [53]. The energy shift of peak A can then be rationalized in terms of dispersion of an electronic state within a crystalline system, providing further evidence for the crystallinity of the Si nanocrystal core. The intensity variation of peak A with excitation energy can be understood if we attribute this feature to the formation of a valence exciton during the x-ray emission process. As shown schematically in figure 2(c), the recombination of an electron at the top of the valence band with a core hole can lead to the formation of a valence exciton *final state* with the electron which had been promoted to the conduction band during photon absorption interacting with the valence band hole. The influence of valence excitons on RIXS has been considered theoretically by Minami and Nasu [54, 55] and by Shirley *et al* [53]. A strong intensity variation of valence exciton features in RIXS can occur when the excitation energy is 'on' or 'off' resonance with the core exciton [53]. When the energy of excitation is 'on resonance', the valence exciton can have much a stronger intensity than the density of states in the valence band due to efficient optical conversion from the core exciton to the valence exciton [53, 54], which agrees well with the observed intensity variation of peak A compared with the valence band as emphasized in figure 6(c). For comparison in figure 6(a) we have put a dotted line at 3.4 eV to denote the X1–X4 valence exciton from bulk silicon; data from [53]. What is particularly striking about the valence exciton in the nanocrystals is the energy range over which the peak can be clearly observed, and its dispersion. Shin *et al* [56] observed a valence exciton feature in bulk Si at 18 K due to Raman scattering resonant with Si $L_{2,3}$ core exciton, but this peak could be observed only within a very narrow excitation energy window (99.30–99.99 eV) and appeared localized in energy. We suggest that the significantly wider energy range over which the valence exciton can be observed in RIXS from the Si nanocrystals in figure 6(a) is due to the enhancement of core exciton formation at the x-ray absorption edge observed in figure 1, which is in turn the result of confinement of the excited electron within the small volume of the nanocrystal. The dispersion observed for the nanocrystal valence exciton feature over the Si $L_{2,3}$ edge indicates that despite the formation of a core exciton as an intermediate state, momentum selectivity in the scattering process does not break down. Carlisle *et al* [57] have suggested that such retention of momentum selectivity in the presence of a core exciton intermediate state arises from the projection of the intermediate state onto a final state which is significantly less localized.

For peak B we did not have enough measurements to draw any significant conclusion because this peak is strongly superimposed on the intense elastic peak and hence not detected. We speculate that peak B may arise from a defect or impurity state. The Si wafer from which the nanocrystals are produced is p-type doped with boron, but at such a low concentration (concentration between $10^{15}$ and $10^{16}$ boron atoms per $cm^{-3}$) that the majority of the resulting nanocrystals will not contain even a single dopant atom. Indeed, the concentration is such that it is unlikely that it would be detected even in a measurement, such as that reported here, which averages over a macroscopic sample. It is, however, possible that unintentional doping may occur during nanocrystal production. Our previous work [8] has shown that only silicon, oxygen and carbon are present in the nanocrystal samples, but it is possible that either the oxygen or carbon (which forms a relatively deep donor state, 0.25 eV below the conduction band minimum in bulk Si) may be present at low concentration within the Si nanocrystal core.

At an incident photon energy of 100.7 eV ($L_2$ edge), figure 5(b), RIXS is most sensitive to Si–Si bonding, so data reflect the LPDOS of Si atoms in the core of the nanocrystals. When the LPDOS of the nanocrystals is compared with that of bulk Si (also measured at the $L_2$ edge for direct comparison—figure 5(a)), it is seen that features within the nanocrystal valence band are as sharp and the total valence band width is smaller (the dash dotted line in figure 3, shows the limit of the Si nanocrystal valence band). The narrower absorption structure in XES from the nanocrystal sample is not seen in bulk Si even at low temperature [56, 58]. In, addition, a low energy tail, peaking at ∼86.6 eV is observed in figure 5(b). In bulk silicon, a similar feature was observed at ∼79 eV [59] due to multielectron transitions ('shake up transitions'). In the case of Si nanocrystals this feature is shifted to higher photon energy due to band narrowing—the valence band in the nanocrystals extends only to ∼87.5 eV (dash dotted line in figure 5), a narrowing of ∼2 eV with respect to the bulk. We attribute the sharper bands in the XES of the nanocrystals and the narrower overall valence band width, to quantum confinement effects in the nanocrystals. The recently reported XES work on silicon clusters in a $SiO_2$ matrix reported by Zimina *et al* [17], do not exhibit the multielectron excitations or valence exciton peak (figure 5(b)). The absence of these features in the data reported in [17] may be due to the quenching of processes which occur in the core or on the surface of the Si cluster by the $SiO_2$ matrix in which the clusters are embedded.

The pronounced core excitonic features in x-ray absorption and valence excitonic features in x-ray emission data makes an accurate determination of band edges, and hence a band gap, extremely difficult. In order to explore the possible effects of quantum confinement on the band gap of the nanocrystals we have collected x-ray excited optical luminescence (XEOL) data for samples prepared by the same procedure [20, 21] as those used in the XAS and XES measurements. The XEOL data were obtained at room temperature (RT) and at 12 K, in order to reduce thermal broadening. Figure 7 shows the emission spectrum of the Si nanocrystal film at RT, acquired with excitation energy of 140 eV. Emission peak positions are found at 430 ± 10 nm (blue) and 620 ± 10 nm (orange) respectively, and it has been suggested that these features originate from oxidized and non-oxidised Si, respectively [24]. In addition to these broad peaks a very sharp feature at 792 nm (1.56 eV), is observed with the same excitation energy (see figure 7, inset), but only at low temperature (there is also possibly a small shoulder at 802 nm, but since the intensity of this feature is comparable to the noise level of the data it will not be discussed further). The sharp feature at 792 nm is assigned to valence exciton recombination in the Si nanocrystal. The presence of the excitonic feature

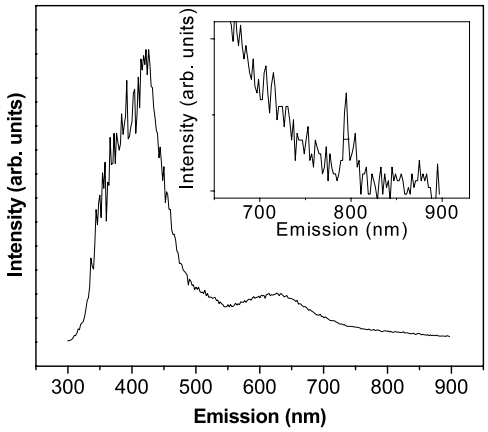


**Figure 7.** XEOL obtained at room temperature (main figure) and 12 K (inset) with an excitation energy of 140 eV.

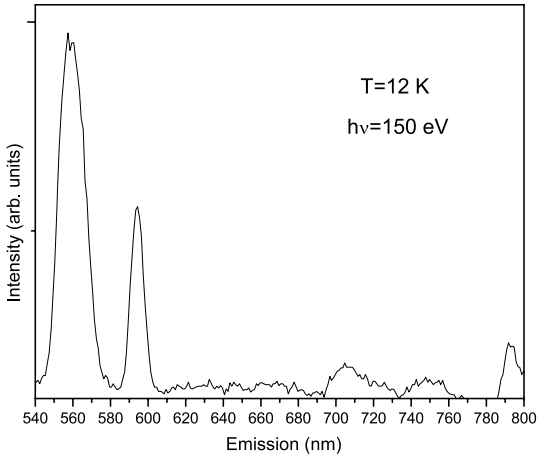


**Figure 8.** XOEL obtained at 12 K with an excitation energy of 150 eV.

at low temperature, where thermal phonon population is low suggests that the band gap in the nanocrystals may be direct, in which case the energy of the excitonic peak provides a minimum value for the band gap of 1.56 eV—substantially larger than the (indirect) gap of bulk Si, 1.11 eV, so providing further evidence for quantum confinement.

In figure 8 the XOEL of SiNCs at 12 K taken with photon energy of 150 eV is presented. Two narrow bands with peak emission, at 594 nm (2.087 eV) and at 558 nm (2.222 eV), and with the full width at half maximum (FWHM) of 8 nm (28 meV) and 17 nm (68 meV), respectively, were observed. The maximum position of the bands correspond to the theoretical values for the PL peaks of oxidized nanocrystals of mean size ∼2 nm and ∼1.6 nm, respectively [60]. The width of the both individual PL peaks is narrow giving the size distribution of the nanocrystals to be ∼±0.1 nm [60]. This is close to the previously reported mean radius values, 2.2 ± 0.4 nm [21].

Although the room temperature PL data reported here agree well with previously reported PL data excited with UV photons (excitation energy 21.2 eV) [24], the position of the luminescence peaks and width at 12 K is different than in our previous report (in this work they are much narrower) [24]. We believe that this is because in this work we have been very careful not to expose the SiNCs to a high flux of the photons at any time in order to avoid possible bleaching effects.

## 4. Conclusions

In this work we have studied XAS, RIXS and XOEL from alkyl-passivated silicon nanocrystals. Emission and absorption spectra show a rich structure associated with electron–hole interactions. The LPDOS measured by RIXS over the Si edge reveal that the LPDOS of the silicon core has discrete atomic-like states which are in agreement with recent PL studies [35]. The overall valence band width is much narrower (by ∼2 eV) than for bulk silicon, which is in accordance with quantum confinement. The XAS data reveal that the edge of the conduction band is masked by core exciton formation and this is why it was not possible to directly obtain the band gap from XAS and XES data. However, with XOEL data we have determined that the band gap energy is not smaller than 1.54 eV. The position and the narrowness of the photoluminescence bands in XOEL when compared with theoretical predictions for oxidized Si nanocrystals [60] reveal that the nanocrystals have mean diameter of ∼2 and ∼1.6 nm, with ±0.1 nm spread in size. This is close to the previously reported mean diameter values of 2.2 ± 0.4 nm obtained from SAXS, AFM, and STM [21].

## Acknowledgments

LŠ is grateful to EPSRC and the EC ARI programme for a financial support. AKC thanks EPSRC and the University of Nottingham for the award of a studentship. SK thanks the ORS and the University of the Newcastle for a studentship. BRH and AH would like to thank EPSRC and CeNAMPS for financial support. We thank Dr NRJ Poolton for helpful comments on the manuscript and for help in making the XOEL measurements.

## References

[1] Dhal J E, Liu S G and Carlson R M K 2003 *Science* **299** 96
[2] Willey T M, Bostedt C, van Buuren T, Dahl J E, Liu S G, Carlson R M K, Terminello L J and Moller T 2005 *Phys. Rev. Lett.* **95** 113401
[3] Wang Y, Kioupakis E, Lu X, Wegner D, Yamachika R, Dahl J E, Carlson R M K, Louie S G and Crommie M F 2008 *Nat. Mater.* **7** 38
[4] Canham L T 1990 *Appl. Phys. Lett.* **57** 1046
[5] Nash K J, Calcott P D J, Canham L T and Needs R J 1995 *Phys. Rev.* B **51** 17698
[6] Gole J L, Dudel F P, Grantier D and Dixon D A 1997 *Phys. Rev.* B **56** 2137
[7] Marsen B, Lonfat M, Scheier P and Saltter K 2000 *Phys. Rev.* B **62** 6892
Sattler K 2002 *Handbook of Thin Films Materials* vol 5 *Nanomaterials and Magnetic Thin Films* ed H S Nalwa (New York: Academic) and references therein

[8] Chao Y, Krishnamurthy S, Montalti M, Lie L H, Kjeldgaard L, Dhanak V R, Hunt M R C, Houlton A, Horrocks B R and Šiller L 2005 *J. Appl. Phys.* **98** 044316

[9] Hoffmann M A, Wrigge G, Issendorff P v, Muller J, Gartefor G and Haberland H 2001 *Eur. Phys. J.* D **16** 9

[10] Eisebitt S, Luning J, Rubensson J-E and Eberhardt W 1999 *Phys. Status Solidi* **215** 803

[11] Kotani A and Shin S 2001 *Rev. Mod. Phys.* **73** 203

[12] Rubensson J-E 2000 *J. Electron Spectrosc.* **110** 135

[13] Eisebitt S, Luning J, Rubenson J-E, van Buuren T, Patitsas S N, Tiedje T, Berger M, Arens-Fischer R, Frohnhoff S and Eberhardt W 1996 *Solid State Commun.* **97** 549
Eisebitt S, Luning J, Rubenson J-E, van Buuren T, Patitsas S N, Tiedje T, Berger M, Arens-Fischer R, Frohnhoff S and Eberhardt W 1996 *J. Electron Spectrosc. Relat. Phenom.* **79** 135

[14] van Buuren T, Dinh L N, Chase L L, Siekhaus W J, Jimenez I, Terminello L J, Grush M, Callcott T A and Carlisle J A 1997 Advances in microcrystalline and nanocrystalline semiconductors *Mater. Res. Soc. Symp. Proc.* 171
van Buuren T, Dinh L N, Chase L L, Siekhaus W J and Terminello L J 1998 *Phys. Rev. Lett.* **80** 3803

[15] Chang G S, Song J H, Chae K H, Whang C N, Kurmaev E Z, Shamin S N, Galakhov V R, Moewes A and Ederer D L 2001 *Appl. Phys.* A **72** 303

[16] Carlisle J A, Dongol M, Germanenko I N, Pithawalla Y B and El-Shall M S 2000 *Chem. Phys. Lett.* **326** 335

[17] Zimina A, Eisebitt S, Eberhardt W, Heitmann J and Zacharias M 2006 *Appl. Phys. Lett.* **88** 163103

[18] Gong X G 1995 *Phys. Rev.* B **52** 14677

[19] Katircioglu S and Erkoc S 2001 *Physica* E **9** 314

[20] Lie L H, Duerdin M, Tuite E M, Houlton A and Horrocks B R 2002 *J. Electroanal. Chem.* **538** 183

[21] Chao Y, Šiller L, Krishnamurthy S, Kjeldgaard L, Patole S N, Lie L H, O'Farrell N, Alsop T A, Houlton A and Horrocks B R 2007 *Nat. Nanotechnol.* **2** 468

[22] Sham T K, Jiang D, Coulthard I, Lorimer J W, Feng X H, Tan K H, Frigo S P, Rosenberg R, Houghton D C and Bryskiewich B 1993 *Nature* **363** 332

[23] Naftel S J, Coulthard I and Antel W 2001 *Appl. Phys. Lett.* **78** 1847

[24] Chao Y, Yang J, Houlton A, Horrocks B R, Hunt M R C, Poolton N R J and Šiller L 2006 *Appl. Phys. Lett.* **88** 263119

[25] Bateman J E, Eagling R D, Horrocks B R and Houlton A 2000 *J. Phys. Chem.* B **104** 5557–65

[26] Sieval A B, van den Hout B, Zuilhof H and Sudholter E J R 2001 *Langmuir* **17** 2172

[27] Wallart X, de Villeneuve C H and Allongue P 2005 *J. Am. Chem. Soc.* **127** 7871

[28] Nordgren J, Bay G, Cramm S, Nyholm R, Rubensson J-E and Wassdahl N 1989 *Rev. Sci. Instrum.* **60** 1690

[29] Kasrai M, Yin Z, Bancroft G M and Tan K H 1993 *J. Vac. Sci. Technol.* A **11** 2694

[30] Hu Y F, Boukherroub R and Sham T K 2004 *J. Electron Spectrosc. Relat. Phenom.* **135** 143

[31] Bianconi A 1979 *Surf. Sci.* **89** 41

[32] Tanaka I, Kawai J and Adachi H 1995 *Phys. Rev.* B **52** 11733

[33] Wu Z Y, Jollet F and Seifert F 1998 *J. Phys.: Condens. Matter* **10** 8083

[34] Brown F C and Rustgi O P 1972 *Phys. Rev. Lett.* **28** 497

[35] Sychugov I, Juhasz R, Valenta J and Linnros J 2005 *Phys. Rev. Lett.* **94** 087405

[36] Brown F C, Bachrach R Z and Skibowski M 1977 *Phys. Rev.* B **15** 4781

[37] Kane E O 1966 *Phys. Rev.* **146** 558

[38] Batson P E and Bruley J 1991 *Phys. Rev. Lett.* **67** 350

[39] Altarelli M and Dexter D L 1972 *Phys. Rev. Lett.* **29** 1100

[40] Suda Y, Obata K and Koshida N 1998 *Phys. Rev. Lett.* **80** 3559

[41] Lu Z, Lockwood D J and Baribeau J M 1995 *Nature* **378** 258

[42] Ma Y, Skytt P, Wassdahl N, Glans P, Mancini D C, Guo J and Nordgren J 1993 *Phys. Rev. Lett.* **71** 3725

[43] Harada Y, Tokushima T, Takata Y, Takeuchi T, Kitajima Y, Tanaka S, Kayanuma Y and Shin S 2004 *Phys. Rev. Lett.* **93** 017401

[44] Tanaka S and Kayanuma Y 1996 *Solid State Commun.* **100** 77

[45] Tanaka S and Kayanuma Y 2005 *Phys. Rev.* B **71** 024302

[46] Benisty H 1995 *Phys. Rev.* B **51** 13281

[47] Bockelmann U and Bastard G 1990 *Phys. Rev.* B **42** 8947

[48] Urayama J, Norris T B, Singh J and Bhattacharya P 2001 *Phys. Rev. Lett.* **86** 4930

[49] Wiech G, Feldhutter H O and Simunek A 1993 *Phys. Rev.* B **47** 6981

[50] Miyano K E, Ederer D L, Callcott T A, O'Brien W L, Jia J J, Zhou L, Dong Q-Y, Ma Y, Woicik J C and Mueller D R 1993 *Phys. Rev.* B **48** 1918

[51] Carlisle J A, Shirley E L, Terminello L J, Jia J J, Callcott T A, Ederer D L, Perera R C C and Himpsel F J 1999 *Phys. Rev.* B **59** 7433

[52] Diaz J, Anders S, Zhou X, Moler E J, Kellar S A and Hussain Z 2001 *Phys. Rev.* B **64** 125204

[53] Shirley E L, Soininen J A, Zhang G P, Carlisle J A, Callcott T A, Ederer D L, Terminello L J and Perera R C C 2001 *J. Electron Spectrosc. Relat. Phenom.* **114–116** 939

[54] Minami T and Nasu K 1998 *J. Electron Spectrosc. Relat. Phenom.* **92** 231

[55] Minami T 1998 *J. Phys. Soc. Japan* **67** 3958

[56] Shin S, Agui A, Watanabe M, Fujisawa M, Tezuka W and Ishii T 1996 *Phys. Rev.* B **53** 15660

[57] Carlisle J A, Blankenship S R, Terminello L J, Jia J J, Callcott T A, Ederer D L, Perera R C C and Himpsel F J 2000 *J. Electron Spectrosc. Relat. Phenom.* **110/111** 323

[58] Eisebitt S, Luning J, Rubensson J E, Settels A, Dederichs P H, Eberhardt W, Patitsas S N and Tiedje T 1998 *J. Electron Spectrosc. Relat. Phenom.* **93** 245

[59] Livins P and Schnatterly S E 1988 *Phys. Rev.* B **37** 6731

[60] Wolkin M V, Jorne J, Fauchet P M, Allan G and Delerue C 1999 *Phys. Rev. Lett.* **82** 197